

Arabidopsis adaptor protein 1G2 is required for female and male gametogenesis

Yongmei Zhou

Fujian Agriculture and Forestry University

Wenqin Fang

Fujian Agriculture and Forestry University

Li-Yu Chen

Fujian Agriculture and Forestry University

Neha Pandey

Fujian Agriculture and Forestry University

Azam Syed Muhammad

Fujian Agriculture and Forestry University

Ray Ming (✉ rayming@illinois.edu)

University of Illinois at Urbana-Champaign <https://orcid.org/0000-0002-9417-5789>

Research article

Keywords: Arabidopsis, AP1G2, megagametogenesis, microgametogenesis, development.

Posted Date: November 12th, 2019

DOI: <https://doi.org/10.21203/rs.2.17134/v1>

License:  This work is licensed under a Creative Commons Attribution 4.0 International License. [Read Full License](#)

Abstract

Background: The gametophytes are essential for the productive process in angiosperms. During sexual reproduction in flowering plants, haploid spores are formed from meioses of spore mother cells. The spores then undergo mitosis and develop into female and male gametes and give rise to seeds after fertilization.

Results: We identified a female sterile mutant from EMS mutagenesis, and a BC1F2 population was generated for map based cloning of the causal gene. Genome re-sequencing of mutant and non-mutant pools revealed a candidate gene, AP1G2. Analyses of two insertions mutants, ap1g2-1 +/- in exon 7 and ap1g2-3 -/- in 3' UTR, revealed partial female sterility. Complementation test using native promoter of AP1G2 restored the function in ap1g2-1 +/- and ap1g2-3 -/- . AP1G2 is a paralog of AP1G1, encoding the large subunit (γ) of adaptor protein-1 (AP-1). ap1g2 mutation led to defective female and male gametophyte development was determined. In the ap1g2 mutants, the mitotic cycles and synchronic development of female gametophytes were impaired, which led to the arrest of female gametophytes at one nucleus stage FG1. Pollen development in ap1g2 was also arrested at one nucleus stage before PMI (pollen mitosis I). AP1G2 was expressed at high levels in different stages of ovule and pollens and actively dividing tissues, including shoot apical meristems, leaf primordial and root tips.

Conclusions: AP1G2 was identified to have a role in the processes of female and male gametogenesis by regulating the first mitosis at one nucleus stage, and the expression pattern suggested AP1G2 is crucial for plant growth and development. Keywords: Arabidopsis, AP1G2 , megagametogenesis, microgametogenesis, development.

Background

Plants have a life cycle alternating between haploid and diploid generation. Flowering plants including *Arabidopsis thaliana* carry female and male gametophytes. The female gametophyte plays an essential role in plant reproduction including guiding the pollen tube, fertilization, and seed development. In Arabidopsis, maize and rice, genetic analysis has revealed that mutant defects were found at all stages of female gametophyte development and analysis of the mutant began to reveal the characteristics of the female gametophyte developmental programs [1-3]. These studies help us understand the regulatory network in the development of female gametophyte [1].

The female gametophyte development occurs over megasporogenesis and megagametogenesis. Most of the angiosperms exhibit the monosporic megasporogenesis pattern. During megasporogenesis, the diploid megasporangium undergoes meiosis and leads to the formation of four haploid megasporangia. Subsequently, generally three micropylar-most megasporangia undergo death and the chalazal-most megasporangium survives, giving rise to a single haploid functional megasporangium. During megagametogenesis phase, the functional megasporangium undergoes a nuclear division with the formation of a two-nucleate embryo sac. The two daughter nuclei separated to the poles by a formed central vacuole, and undergo a second karyokinesis forming a four-nucleate embryo sac. With the vacuole increased in size, a third syncytial cell division undergoes resulting a large eight-nucleate coenocytic cell. Two polar nuclei migrate from each pole to fuse with the formation of a diploid central nucleus, followed by cellularization and cell differentiation, thus generating a mature female gametophyte consists of three antipodal cells, two synergic cells, one egg cell, and one central cell [2, 4, 5].

Large-scale screens for female sterile mutants have identified hundreds of female gametophyte mutants and most mutants in these screens also exhibited defects in the male gametophyte. Most of the characterized genes mediate essential functions [1, 2, 6]. Screening for female sterile mutants is a challenging task as it requires one additional generation to identify female sterile mutants. It also takes one additional generation to make crosses because such mutants can only be maintained in heterozygous genotype. Our objective is to build a collection of female sterile mutants ranging from inception of carpel primordia, abortion of female reproduction organ, to pre- and post-meiosis mutations affection female gametophyte development to explore gene network controlling sex determination in male flowers.

We identified the role of AP1G2 in female and male gametogenesis by map based cloning, which encodes a large subunit of AP-1(adaptor protein complex-1). Adaptor protein (AP) complexes, the predominant coat proteins linking the membrane proteins with clathrin molecules that form the coat of a lipid vesicle, have been characterized in various eukaryotic cells. They interact with membrane proteins such as different class of cargo receptors in the process of generating a clathrin-coated vesicle (CCV). The structure of AP complexes is highly conserved across all eukaryotes and comprise two large subunits ($\alpha/\gamma/\delta/\varepsilon$ and β), one medium μ

subunit and one small σ subunit, and lack of any single APs subunit impairs the function of APs [7-9]. Among the APs, AP-1 plays a role in soluble enzyme composition and some membrane proteins from trans-Golgi network (TGN) to endosomes and lysosomal transport [10-12]. The γ subunit of AP-1 is encoded by *AP1G1* and *AP1G2* [13]. Earlier studies demonstrated that AP1G is crucial for synergid-controlled pollen tube reception and pollen development through mediating vacuolar remodeling [12, 14]. Here, the new functions of *AP1G2* were characterized in regulating gametogenesis.

Results

Mutant with defects in ovule development

We obtained a female sterile mutant from an Ethyl methanesulfonate (EMS) mutagenesis screening. The mutant showed increased flower size than the wild-type and shorter siliques with no seed set (Fig. 1A-D). Cytological observation showed that compared with the ovule development in wild-type plants (Fig. 2A-E), the outer integument development of mutant was arrested (Fig. 2G). The mutant had defects in integument development, presented embryo sac development partially arrested at stage FG1 [15] in which the functional megasporangium either persisted or degenerated after FG1 stage (Fig. 2K,L), the functional megasporangium of around 43.70% ovules could still undergo three times mitosis and develop into mature embryo sacs (Fig. 2J). After two rounds of backcrosses to reduce genetic background, the mutant showed very low seed setting rate. The seeds had thin endotesta, but no episperm that should have developed from outer integument to serve as hard dry protective covering (Fig. 1E, F). The seed set(11.11%, n=432) was lower than the percentage of the ovules contained normal female gametophytes, indicating the reduction was probably caused by aberrant outer integuments. Despite of the absence of outer integuments, a few of these malformed seeds were still able to germinate in soil.

Mutation identification

After backcross to wild-type (WT) plants, the self-pollinated BC1F2 plants were analyzed. The segregation ratio wild type to mutant fits the expected 3:1 ratio (Chi-Square=0.140, df=1, P=0.708), indicating that this mutation is recessive. After backcrossing to WT, BC1 individuals were self-pollinated and DNA of 40 BC1F2 plants of mutant and non-mutant were pooled separately for whole genome sequencing as described by Nordstrom [16]. We compared a causative mutation based on the frequency of the non-reference allele of a SNP (Single Nucleotide Polymorphisms) in the mutant and the non-mutant pools. If the non-reference allele of a SNP is the causal mutation, its frequency in the mutant pool should be 100% and about 33% in the non-mutant pool, and the SNPs associated with the causal gene should also displayed the high frequency of non-reference alleles in the mutant pool [17]. We selected 95 candidate SNPs (0.6% of total SNPs) with the frequency higher than 90% and lower than 50% in the mutant and non-mutant pools respectively (Fig. 3A). Among the 95 candidate SNPs, 81.05% of them were on chromosome I, 0.07% on chromosome II, 0.06% on chromosome III, 0.02% on each chromosome IV and chromosome V. Closer inspection of SNPs on chromosome I, we selected SNPs (30 associated genes) in coding regions caused non-synonymous mutations or located in UTR (Untranslated Regions) for further analysis in the backcross BC2 progeny. As recombination events of the SNPs linked to the causal gene, each SNP was confirmed by PCR and sequencing at least 12 mutants separately in BC2 progeny. We found only At1g22730 and At1g23900 had 100% frequency of non-reference allele in mutants, and At1g22410 had frequency of 96%, making At1g22410, At1g22730 and At1g23900 candidate genes of the sterile mutant (Fig. 3B, C).

Confirmation of candidate genes of female sterile mutant

To determine which casual gene was associated to the sterile mutant, we ordered several mutant lines with T-DNA insertion in each candidate gene(Fig .S2). Among the T-DNA insertion lines, two lines with the insertion in *AP1G2*(At1g23900) showed phenotype of reduced seed set. The mutant *ap1g2-1* (SALK_032500) with T-DNA insertion in exon7, its heterozygote had 51.9% seed set and almost half of the ovules were aborted (Fig .4A-C). For *ap1g2-3* (SALK_137129) with T-DNA insertion in 3'UTR, 56bp upstream from poly A tail of the mRNA, homozygous plants (*ap1g2-3'*) was obtained with 23.27% of seed set (Fig .4A-C). To test whether the mutant phenotype could be restored spontaneously, 5 self-pollinated progenies of *ap1g2-3'* was checked. The result showed their seed set had no significant difference to each other (Fig S3).

Reciprocal crosses were carried out to determine whether the *ap1g2* mutation affected the female or male gametophyte. *ap1g2-1^{+/−}* was used to pollinate the wild-type plants, or used as female parent for pollination with wild-type pollens. And the seeds from *ap1g2-1^{+/−}* were grown in soil. The genotypes of all progeny plants were assessed by PCR and scored (Table 1). The progeny of the self-pollinated *ap1g2-1^{+/−}* exhibited a 1:1 segregation of the wild type to *ap1g2-1^{+/−}* plants (Chi-Square=0.342, df=1, P=0.559), and no homozygotes were recovered. When *ap1g2-1^{+/−}* was used as the female and male parent, the transmission efficiency was 63.63% and 60.47%, respectively. Both female and male transmission were decreased. However, in spite the partial penetrance for the *ap1g2-1* allele, homozygotes for the mutation were never identified. The seeds from *ap1g2-1^{+/−}* and wild-type plants were germinated on MS medium. After 2 weeks, we counted the number of seedlings and seeds failed to germinate. The analysis showed the seed germination rate of *ap1g2-1^{+/−}* progeny had no significant difference with the wild-type (Pearson Chi-Square=0.668, df=1, P=0.414).

To obtain heteroallelic homozygous mutants, we crossed *ap1g2-1^{+/−}* as egg donors and *ap1g2-3^{−/−}* as pollen donors. In the offspring, only *ap1g2-1/ap1g2-3* showed the phenotype of reduced seed set with fruits containing 47.75% normal seeds, while heterozygous plants *ap1g2-3^{+/−}* had no fertility reduced phenotype.(Fig .4B, C). These data supported that the insertion in 7th exon of *AP1G2* had stronger defect than that in 3'UTR. Since *ap1g2-3* mutation was in untranslated region, and our RNAseq data of ovules at stage FG1 from *ap1g2-3*, *ap1g2-1^{+/−}* and *ap1g2-1/ap1g2-3* showed *AP1G2* transcription level of *ap1g2-1/ap1g2-3* was higher than *ap1g2-3^{+/−}* (unpublished data), and similar to *ap1g2-1*, indicating other factors might affect *AP1G2* transcription of *ap1g2-3* allele.

To confirm that *ap1g2* was responsible for the fertility reduced phenotype, we carried out complementation test using native promoter (*ProAP1G2*) driven wild type *AP1G2* allele. 5 of 19 independent lines that are heterozygous for *ap1g2-1* and carried the transgene showed a higher seed set (70.55%). For *ap1g2-3^{−/−}*, 26 independent lines were obtained, and 8 lines complemented the *ap1g2-3^{−/−}* phenotype. The seed set of the *ap1g2-3^{−/−}* carrying the construct *ProAP1G2:AP1G2* was 90. 81%, approaching that of WT (Fig .4B, C). And genetic complementation lines of *ap1g2-4^{−/−}* also could partially rescue fertility reduced phenotype (Fig .S5). Altogether, these data suggested that the reduced fertility was due to the mutations in the *AP1G2* (Fig 4B).

Developmental stage of female gametophyte affected by *ap1g2*

To understand at which stage the megagametophyte development might be affected in the *ap1g2* mutants, around whole-mounted cleared 2000 ovules from WT, *ap1g2-3^{−/−}* and *ap1g2-1^{+/−}* at different stages of development were analyzed. The results showed that the outer integuments developed normally in wild-type plants and *ap1g2* mutants and these plants were all able to produce normal functional megasporangium (Fig .5A, F, L). Thereafter at stage FG3, wild-type plants contained a two-nucleate embryo sacs, and continued to develop, producing four-nucleate embryo sacs and then mature embryo sacs (Fig .5B, C, D, E).While in plants *ap1g2-3^{−/−}*, most of the ovules remained a single cell in the nucellus or degenerated gradually (Fig .5G-J). And about 50% of the ovules from *ap1g2-1^{+/−}* were arrested at stage FG1 with the functional megasporangium persisting or degenerating during development. We observed 989 ovules in *ap1g2-1^{+/−}* mutant, and the number of aborted ovules as described above was half of total number (1:1, Chi-Square=0.171, P=0.679).

As all the impaired embryo sacs observed in EMS-induced mutant (*ap1g2-4^{−/−}*), *ap1g2-3^{−/−}* and *ap1g2-1^{+/−}* were arrested at one-nucleus stage (Table 3), we concluded that these defective female gametophytes were due to the loss *AP1G2* function. And ovules in both insertion alleles, *ap1g2-1^{+/−}* and *ap1g2-3^{−/−}* were all able to fully develop outer integuments, but complementation lines of *ap1g2-4^{−/−}* still had the defect of outer integuments, suggesting the defective outer integuments in *ap1g2-4^{−/−}* were affected by other mutations induced by EMS rather than the mutation in *AP1G2*.

To confirm the cell that persisted in the abortive ovules was functional megasporangium, the *ANTI-KEVORKIAN (AKV)* cell-identity marker during megagametogenesis were used, [18]. The promoter pAKV is a gametophyte-specific promoter, and pAKV:H2B-YFP marker specifically expressed in the nuclei of the functional megasporangium and the developing gametophyte before cellularization [19]. *ap1g2-1^{+/−}* and *ap1g2-3^{−/−}* plants were crossed with pAKV:H2B-YFP marker lines. We then analyzed plants with *ap1g2-1^{+/−}* allele and F2 plants with *ap1g2-3^{−/−}* allele which were partially sterile. The functional megasporangia were formed normally in both *ap1g2-1^{+/−}* and *ap1g2-3^{−/−}* (Fig .5L). But after FG1, when the wild-type ovules performed first nuclear division, producing a two-nucleate embryo sac, the defective embryo sacs from two mutants still stayed at stage FG1 instead of completion of mitotic divisions (Fig .5M-O).

The female gametophyte development within a pistil is generally synchronous with a relative narrow range of variation in WT [20, 21]. To investigate the developmental synchrony of female gametophytes in the pistils of *ap1g2* mutants, we emasculated the stage 12 flowers, and after 48-72 h, we fixed pistils from flowers of the wild type and mutants at different developmental stages. The pistils from the same inflorescence were sequentially opened, and each ovule in a pistil was examined for their development stages. Compared with wild-type pistils, we observed that the developmental synchrony of female gametophytes in *ap1g2-1^{+/−}*, *ap1g2-3^{−/−}* and *ap1g2-4^{−/−}* mutant was not only disturbed but delayed the progression of nuclear division as shown in table 2-3. In *ap1g2-1^{+/−}* pistils, about half of the female gametophytes in each mutant pistils (P9-P14) were either persisted at FG1 or degraded and approximately half were wild type. While in the *ap1g2-3^{−/−}* and *ap1g2-4^{−/−}*, around 77.75% and 57.3% of the female gametophytes were found failed to undergo nuclear division. The numbers of aborted ovules detected in *ap1g2-1^{+/−}* and *ap1g2-3^{−/−}* were very close to the aborted seed rates correspondingly, which suggested that the disruption in megagametogenesis was the main factor of the reduced seed set in *ap1g2* mutants.

Developmental stage of male gametophyte affected by *ap1g2*

To analyze whether the mutation led to additional male abortion phenotype, the viability of pollens was tested using Alexander staining. 46.04% (n = 2096) non-viable pollen was detected in mature anthers in *ap1g2-1^{+/−}* plants (Fig .7F, H), and 49.71% non-viable pollen was obtained for *ap1g2-3^{−/−}* plants (n = 1750). However, in *ap1g2-1^{+/−}* carrying the construct proAP1G2:GUS, the viability rate was 71.22% (n=300), and in *ap1g2-3^{−/−}* plants carrying the transgene, viability rate reached similar level as the wild type, resulting in 1.64% (n=600) aborted pollen, respectively.

In *Arabidopsis*, the development of the male gametophyte begins with the expansion of the microspore (Fig .6A, B) and a large vacuole produced, accompanied by the microspore nucleus moving to a peripheral location against the cell wall. The microspore then undergoes the first asymmetric pollen mitosis(PMI) which results a bicellular pollen grain with a large vegetative cell engulfing a small germ cell in the cytoplasm (Fig .6C). After PMI, the smaller germ cell undergoes the second mitosis (PMII) to produce twin sperm cells (Fig .6D). Therefore, a mature pollen grain consists of a vegetative cell and two sperm cells [22-24].

In order to understand how the *ap1g2* mutation affected pollen viability, 4',6-diamidino-2-phenylindole (DAPI) staining was used to analyze pollen development in wild-type plants and *ap1g2-1^{+/−}*. The normal mature pollen grains from wild type and *ap1g2-1^{+/−}* showed three nuclei, including one vegetative nucleus and two generative nuclei (Fig .6I, J). While nearly half of the pollens from *ap1g2-1^{+/−}* could not detect nuclear fluorescence signal in abnormal pollens showing shriveled shape (Fig .6J).Though at microspore stage, pollens in both WT and *ap1g2-1^{+/−}* showed normal single nucleus fluorescence (Fig .6K, L), nearly half microspores of *ap1g2-1^{+/−}* were not observed nuclear polarization before pollen mitosis but still showed unicellular and shriveled microspores (Fig .6O, P) at stage 12 when tricellular pollens had formed in the wild type (Fig .6M, N).

Half the pollens from *ap1g2-3^{−/−}* under scanning electron microscopy (SEM), showed to be wrinkled shaped (Fig .7B, D), in contrast to those of wild type (Fig .7A, C). Besides, solid pollen germination medium [25] were used with the pollens from WT and *ap1g2-3^{−/−}*, and we obtained 72.22% (n=180) and 30% (n=180) germination respectively (Fig .7E, F).

AP1G2 expression pattern

Analysis of mutation in *AP1G2* showed that *AP1G2* is of importance for the development of both the female and male gametophyte. To characterize *AP1G2* expression in plants, we analyzed *AP1G2* expression using qRT-PCR and reporter gene expression experiments.

Total RNA was isolated from different organs. And specific primers were used to detect *AP1G2* mRNA, *Actin* (*Act2*, *At3g18780*) as an internal control. The qRT-PCR analysis revealed that *AP1G2* expression was present in each organ selected from wild-type plants, including roots, leaves, stems and flowers, but the relative expression in flowers was the highest, followed by stems and leaves that were about half of the level of *AP1G2* expression in flowers (Fig .8). And for *ap1g2-3^{−/−}* mutants with the T-DNA insertion in 3'UTR, the expression levels were significantly down-regulated compared with the wild-type using t-test (P<0.01).

Expression pattern was analyzed in transgenic plants to study the temporal and spatial profiles of *AP1G2* gene expression. A construct in which 2 kb upstream of *AP1G2* of the start codon was fused with the GUS reporter gene was transformed into the wild-type plants. 23 independent lines of T2 generation were analyzed, of which 5 showed GUS expression in the female gametophyte and GUS expression was detected after the big vacuole formed (Fig .9C) and remained until embryogenesis began, after which GUS staining reduced (Fig .9C-F). And it seemed to show the same pattern in anthers, Pro*AP1G2*:*GUS* notably expressed in the male gametophyte at maturation in all independent lines we observed (Fig .9G-I). Additionally, pro*AP1G2*:*GUS* was expressed in the 8-10 days seedling stage, and expression was also noted in hypocotyle (young shoot), leaves and flowers including expression in anthers, filament, pedicles, leaf primordial and shoot apical meristem. GUS expression was also observed in root tips, strong GUS staining was noted in trichomes (Fig .S4).

Discussion

After mapping the causal mutation of a sterile mutant obtained from EMS mutagenesis, screening, and annotation of candidate SNPs, the three genes At1g22410, At1g22730 and At1g22930 showed approaching 100% of frequency of non-reference alleles in the mutant pool due to the suppression of recombination events of the identified loci [26]. Confirmation of candidate genes was performed by studying single mutants of each candidate gene and we found the phenotype of T-DNA insertion lines of At1g23900 (*AP1G2*) was very close to our mutant especially in terms of female sterility.

AP1G1 and *AP1G2* are homologous genes, and both encode γ subunits of a heterotetrameric protein complex (AP-1) that sorts proteins at the trans-Golgi network and endosomes [12, 13]. Previous studies on single mutants of both genes did not show an observable phenotype, while functional loss of both genes resulted failure of pollen tube discharge and synergid degeneration and male lethality, accompanied with defective vacuolar dynamics and acidification [12, 14]. In this work, the new function of *AP1G2* was characterized. Since both *ap1g2-1^{+/−}* and *ap1g2-3^{−/−}* mutants showed that partial female and male gametophytes were arrested at one-nucleus stage, and complementation test using promoter *ProAP1G2* restored the phenotype of reduced fertility in *ap1g2-1^{+/−}* and *ap1g2-3^{−/−}*. We concluded that *AP1G2* played a crucial role in the processes of female and male gametogenesis by regulating mitosis of micro- and mega-gametogenesis at one-nucleus stage.

For *ap1g2-1^{+/−}* and *ap1g2-3^{−/−}*, their severe degree of defect was different due to their different insertion position. A similar effect was also observed in *kin-1a* and *kin-1C/c* mutant[27].The mutant *ap1g2-1^{+/−}* with T-DNA insertion in exon 7 which caused frame shift mutations, about half of its female gametophyte development was arrested in heterozygous genotype. While for *ap1g2-3* with insertion in 3'UTR (56bp upstream from poly A tail of mRNA), only homozygous plants (*ap1g2-3^{−/−}*) were defective in female gametophyte development, but the seed set and percentage of normally developing female gametophytes were significantly lower than those of *ap1g2-1^{+/−}*, suggesting that the defect of *ap1g2-3* was not strong as *ap1g2-1* allele . By comparing the expression levels between WT and *ap1g2-3^{−/−}*, we found insertion mutation in 3'UTR of *AP1G2* decreased the gene's own expression in various organs. This result supports that mutation within the 3'UTR can decrease translation efficiency of the mRNA [28, 29]. *ap1g2-1^{+/−}* showed 1:1 segregation after selfing, no homozygotes obtained, which seems to be gametophytic defect. But both embryo scs and pollens of *ap1g2-1^{+/−}* showed about 60% transmission efficiency, which means about 60% of normal gametophytes also carried *ap1g2-1*. Therefore, *ap1g2-1* is a leaky allele, not a strict gametophytic defect[30]. The information that determine functional megasporangium whether undergo mitosis,was likely from sporophytic tissues around the gametophytes.We speculate both female and male gametes underwent gametic selection, stringently avoided to produce homozygous *ap1g2-1* plants during the process of fertilization. Thus, we suspect sporophytic functions of *ap1g2* affected gametophyte development and even gametic selection. *ap1g2-4* is a single base mutation in the 7th exon of *AP1G2*. This defectionwas not strong as *ap1g2-1* or *ap1g2-3*, because homozygous *ap1g2-4* allele caused only about 50% aborted ovules, lower than *ap1g2-3* homozygous plants. Previous work showed *AP1G1* and *AP1G2* function redundantly in male gametophyte development[12]. So another γ isoform function in male gametophyte developmet. Considering that the two factors might counteract the mutation effect and complementation lines could partially rescue seed abortion, we conclude that *ap1g2-4* mutation affected *AP1G2* function in female gametophyte development. As for the additional outer integuments defect, our RNAseq data showed *INO* (*INNER NO OUTER*) transcription level was down-regulated in *ap1g2-4* mutant, but had same level in T-DNA insertion lines and wild-type plant(unpublished data). *INO* was known to be associate ith outer integument initiation[31], and the

phenotype of *ino* were extremely similar to *ap1g2-4* mutant. Therefore, this additional defect was due to other mutations which might be upstream regulators of *INO*.

A previous study reported that *AP1G2* were expressed throughout the plant [12]. We examined the expression pattern of *AP1G2* using qRT-PCR and reporter gene expression. *AP1G2* expression was higher in florescence than that of roots, leaves and stems.

Pro*AP1G2:GUS* transgenic plants showed high expression level of *AP1G2* in male gametophyte, and the level was increased as the male gametophyte developed. We obtained 5 independent lines with GUS staining in female gametophyte from 23 lines. In these 5 lines, GUS expression was detected in entire embryo sac after the large vacuole formed rather than in synergid cells, and remained expressed until embryogenesis began. These results indicated that *AP1G2* functions during female and male gametophyte development.

In *ap1g2-1^{+/−}* and *ap1g2-3^{+/−}* mutants, about half of the microspores were found without the central nucleus migration to a peripheral position against the cell wall by a large vacuole and undergoing an asymmetric cell division (PM I). Coincidentally, in defective embryo sacs of *ap1g2*, the first mitosis did not occur nor did it form a large vacuole, suggesting that the mutation might affect a similar process in both gametophytes. But we understand little about the inner mechanisms. The phenotypes of *ap1g2* were similar to the insertion lines in *VACUOLELESS GAMETOPHYTE* (VLG) [23]. VLG was found localized in plant prevacuolar compartments (PVCs) or multivesicular bodies (MVBs), which mediate the transport of proteins into vacuoles in the secretory pathway and were also considered as late endosomes in the endocytic pathways. The cytosolic adaptor protein-1 complex (AP-1) that were found on the TGN/endosomal membranes also plays an essential role in protein trafficking between the TGN and endosomes by specific sorting signals [10-12]. This suggested that post-Golgi traffic pathway is crucial to gametophyte development.

Reports for AP-1 complex indicate that AP-1 is required for viability in multicellular organisms. In mice, homozygous destructions of the genes encoding $\gamma 1$ or $\mu 1A$ lead to embryonic lethality [32, 33]. Deficiency of AP-1 is synthetically lethal in yeast with a temperature-sensitive clathrin heavy chain in *Saccharomyces cerevisiae* [34] and a removal of calcineurin, which is a regulator of Ca^{2+} signaling in *Schizosaccharomyces pombe*, lead to pleiotropic defects in cytokinesis, cell integrity, and vacuole fusion in fission yeast [35]. In Arabidopsis, the medium subunit of AP-1, redundant AP-1 μ -adaptins AP1M1 and AP1M2, were reported to form a complex with large subunits γ -adaptin of the heterotetrameric AP-1. The knockout mutation *ap1m2* displayed impairing pollen function and arrested plant growth, and *ap1m1ap1m2* double mutant was nearly pollen-lethal [13]. Analysis of a double knockout *ap1g1 g2^{+/−}* indicated AP1G is important to synergid-controlled pollen tube reception and pollen development by mediating vacuolar remodeling [12, 14]. However, our results pointed to an importance role of female and male gametophyte development, indicating that *AP1G1* and *AP1G2* function redundantly in pollen tube discharge and male gametophyte development, but the later one has its distinct role in female gametophyte development. And *AP1G2* might be more important to male gametophyte development, since single *ap1g1* mutant did not show observable defects [12, 14]. Though we know little about the relation either between AP1M1 and AP1M2, or AP1G1 and AP1G2, analysis of double knockout *ap1m1ap1m2* and *ap1g1 g2^{+/−}* revealed that both AP1M and AP1G play an important role in pollen function and plant growth in Arabidopsis. Current studies indicate that AP-1 is necessary for the correct performance of somatic cytokinesis in root and shoot cells in Arabidopsis [7]. AP1M1 promotes secretory and vacuolar trafficking, which is essential for cell division and growth during both pollen development and plant growth [13]. However, *AP1G2* expression was also detected in the shoot apical meristems, leaf primordial and root tips where cell division is active, suggesting its function is beyond the gametophyte stage and crucial for plant growth.

Conclusion

The new functions of *AP1G2* were characterized in Arabidopsis. *ap1g2* mutation led to defective female and male gametophyte development was determined. In the *ap1g2* mutants, the mitotic cycles and synchronic development of female gametophytes were impaired, resulting in the arrest of female gametophytes at one nucleus stage FG1. Pollen development in *ap1g2* was also arrested at one nucleus stage. *AP1G2* was expressed at high levels in different stages of ovule and pollens and actively dividing tissues, including shoot apical meristems, leaf primordial and root tips, suggesting the function of *AP1G2* is beyond gametophyte development.

Materials And Methods

Plant materials and growth condition

The T-DNA insertion lines of *AP1G2*, SALK_032500 (*ap1g2-1*), SALK_137129 (*ap1g2-3*), and lines of At1g22410, and At1g22730 in Fig S2 were obtained from the Arabidopsis Biological Resource Center (ABRC) . The pAKV:H2B-YFP marker line was kindly provided W.C. Yang. All of the seeds were sterilized with 75% ethanol, cold-treated at 4°C overnight, germinated in Murashige and Skoog (MS) medium, and seedlings were planted in an air-conditioned room under a photoperiod (L : D = 16 h:8 h) at 22°C.

Mutant screening and next-generation sequencing analysis

The wild type and mutants used were all of Columbia ecotype. Wild-type seeds were mutagenized with 40 m EMS for 8 hours, and mutants induced by EMS were identified by screening plants of the second generation. The identified female-sterile mutants were backcrossed to the wild-type to generate BC1 progeny and propagated by self-pollination to generate BC1F2 segregating population.

The equal amount of genomic DNA extracted from leaves of mutant plants and non-mutant plants were pooled. The libraries of both pools were constructed and sequenced by Illumina HiSeq™2500 platform at Novogene Corporation. The average sequencing depth was about 32× coverage for both mutant and nonmutant pools. The reads we obtained from mutant and non-mutant pools were aligned to the Col-0 reference genome (Arabidopsis_thaliana.TAIR10.21) by the software BWA, and SAMtools-mpileup was used to identify potential SNPs as described [17]. Single nucleotide polymorphisms (SNPs) of mutants was detected among BC1F2 segregants. Each candidate SNP was confirmed by PCR and sequencing at least 12 mutants separately in BC2 progeny using primers as listed in Fig S1.

PCR-based screening of T-DNA insertions

Molecular identification of genotype of the T-DNA insertion lines was performed as described [36]. The primers used for identification were designed by online tool (<http://signal.salk.edu/tdnaprimers.2.html>). For *ap1g2-1*, T-DNA-specific primer LBb1.3 (5'-ATTTGCCGATTCGGAAC-3') was used to determine the genotype by PCR combined with the specific primers on genomic sequence, *ap1g2-1RP* (5'-actttgttatcctgggttcttg-3') and *ap1g2-1LP* (5'-GAGCTCAAGAAGCAACAATCC-3'). For *ap1g2-3*, the genotype was determined by PCR using the LBb1.3 combined with *ap1g2-3RP* (5'-TTATGAATTTCGCATCAAGCC-3') and *ap1g2-3LP* (5'-GAGTCACTAACAGCCAGCAGG-3'). For the other two candidate genes, the genomic sequence-specific primers were included in Fig S2.

qRT-PCR

Total RNAs were extracted from different organs using Total RNA Kit I (OMEGA). The first-strand cDNA synthesis for Real-time PCR and the later were respectively performed using PrimeScript® RT reagent Kit and SYBR Premix Ex Taq™ (Takara). Real-time RT-PCR was performed with using primers AP1G2q-F (5'-CTCCTGGCAAGCGGTAGT-3'), AP1G2q-R (5'-GCGAGGGAAGTTGCTGAC-3') for AP1G2 and Actin2F (5'-TCCCTCAGCACAT

TCCAGCAGAT-3') and Actin2R (5'-AACGATT CCTGGACCTGCCTCATC-3') for the reference gene *ACTIN2*.

Seed set and fertility analysis

To analyze the seed set of the wild-type and mutants, the total number of ovules and seeds contained in the first 7-15 siliques on the primary inflorescence were counted, as described [37]. We used 10 plants per genotype to comparing the seed set. For megagametophyte analysis, ovules were excised from different-sized pistils previously fixed in FAA (70% ethanol: acetic acid: 30% methyl aldehyde, 9:0.5:0.5). They were cleared with chloral hydrate solution (chloral hydrate: glycerol: sterilized water, 8:1:2) and examined with the Olympus BX63 microscope equipped with DIC and phase-contrast optics. The seed set in each siliques was the percentage of seeds to the total number of ovules. Statistical significance of the values using One-Way ANOVA, followed by a LSD (Least Significant Difference) test.

Vectors Construction

The genomic region ~ 2kb before the start codon ATG corresponding to the putative AP1G2 promoter was amplified by PCR from wild type genomic DNA using proAP1G2-F (CACCAATACATGAGGGAAAGGTGAGA) in combination with the reverse primer proAP1G2-R (TTGGTCCACCGGCAACTTTA). For the molecular complementation test, the 7912bp of genomic fragment containing the promoter and gene of *AP1G2* was amplified by PCR using the forward primer proAP1G2-F, in combination with the reverse primer AP1G2-R (CAACCCGCGAGGGAAAGTTG) upstream of the stop codon. All PCR products were cloned in the pENTR/D/TOPO vector (Invitrogen). The generated entry vectors were subsequently used for generating the corresponding expression vectors PGWB533-GUS.

Plant transformation

Arabidopsis plants were transformed with agrobacterium tumefaciens strains GV3101 using floral dip method [38]. The presence of the transgene in T1 plants was confirmed by PCR using forward primer pro-F (agttagagttaggtacgtcagaa) for transgenic lines with promoter and gene-F (ACGGAAAAGATGTATTAGAGG) for complementation lines, and combined with the reverse primer GUS-R (CGCGAAATTCCATACCTG).

Histology and microscopy

For phenotypic analysis, The whole inflorescences from wild type and *ap1g2* mutants were fixed in FAA fixative solution overnight, and transferred to sterilized water for 2min. The ovaries were dissected on a slide and cleared in chloral hydrate solution and finally photographed using Olympus BX63 microscope equipped with DIC and phase-contrast optics. For β-Glucuronidase (GUS) staining, GUS histochemical assays kit (Real-Time, China) was used following the manufacturer's protocol. Inflorescences and developing seedlings were incubated in GUS staining buffer at 37°C overnight. Ovules were then washed in 75% ethanol for 7 h, repeat 3 times for examination and photographs. To test the viability of the pollen, the anthers were collected at anthesis stage and evaluated by staining with Alexander (Solarbio). The development stage of pollen in wild type and mutants was analyzed for each subsequent bud in the same inflorescence from an open flower to the next 10 unopened buds. Anthers were placed on slides with DAPI staining solution (0.02 M citric acid, 0.16 M Na₂HPO₄, 0.2μgml⁻¹ DAPI (Sigma-Aldrich) [23].

Confocal microscopy of ovules

To confirm that megagametogenesis was affected in *ap1g2* ovules, *ap1g2-1*^{+/−} mutant plants were crossed with pAKV:H2B-YFP marker lines. We then analyzed five progenies with an *ap1g2-1* allele that showed partial sterility. The ovules at different flower stages

were observed using a Leica TCS SP8X confocal microscope at an excitation wavelength of 488 nm. Emissions were collected at 500-530 nm to visualize yellow fluorescence protein (YFP). Anthers for each successive bud mounted into slides with DAPI staining solution were also observed using the confocal microscope at an excitation wavelength of 405 nm and emissions were collected at 415 nm-500nm.

Declarations

Acknowledgements

This work was supported by the grant 2015N20002-1 from the Department of Science and Technology of Fujian Province to RM, National Science Foundation (NSF) Plant Genome Research Program Award DBI-1546890 to R.M.

1. Ethics approval and consent to participate: Not applicable
2. Consent for publication: Not applicable
3. Availability of data: The data sets used or analysed during the current study are available from the corresponding author on reasonable request..
4. Competing interests: The authors declare that they have no competing interests.
5. Funding: This work is supported by the grant 2015N20002-1 from the Department of Science and Technology of Fujian Province to RM, National Science Foundation (NSF) Plant Genome Research Program Award DBI-1546890 to R.M.
6. Authors' contributions: RM conceived the project, ZYM and FWQ generated the data, ZYM analyzed and interprets the data. ZYM wrote the manuscript. RM, CLY, NP and SMA revised the manuscript.
7. Acknowledgments: Not applicable.

References

1. Yadegari R, Drews GN: **Female Gametophyte Development**. *The Plant cell* 2004, **16**(suppl 1):S133-S141.
2. Drews GN, Koltunow AM: **The female gametophyte**. *The arabidopsis book* 2011, **9**:e0155.
3. Cucinotta M, Colombo L, Roig-Villanova I: **Ovule development, a new model for lateral organ formation**. *Frontiers in Plant Science* 2014, **5**(117).
4. Maheshwari P: **An introduction to the embryology of angiosperms**. In.: McGraw-Hill; 1950.
5. Yang WC, Shi DQ, Chen YH: **Female gametophyte development in flowering plants**. *Annual review of plant biology* 2010, **61**:89-108.
6. Pagnussat GC, Yu HJ, Ngo QA, Rajani S, Mayalagu S, Johnson CS, Capron A, Xie LF, Ye D, Sundaresan V: **Genetic and molecular identification of genes required for female gametophyte development and function in Arabidopsis**. *Development* 2005, **132**(3):603-614.
7. Teh OK, Shimono Y, Shirakawa M, Fukao Y, Tamura K, Shimada T, Hara-Nishimura I: **The AP-1 μ adaptin is required for KNOLLE localization at the cell plate to mediate cytokinesis in Arabidopsis**. *Plant Cell Physiol* 2013, **54**(6):838-847.
8. Bonnemaison ML, Back N, Duffy ME, Ralle M, Mains RE, Eipper BA: **Adaptor Protein-1 Complex Affects the Endocytic Trafficking and Function of Peptidylglycine alpha-Amidating Monooxygenase, a Luminal Cuproenzyme**. *The Journal of biological chemistry* 2015, **290**(35):21264-21279.
9. Navarro Negredo P, Edgar JR, Wrobel AG, Zaccai NR, Antrobus R, Owen DJ, Robinson MS: **Contribution of the clathrin adaptor AP-1 subunit micro1 to acidic cluster protein sorting**. *The Journal of cell biology* 2017, **216**(9):2927-2943.
10. Bonnemaison M, Back N, Lin Y, Bonifacino JS, Mains R, Eipper B: **AP-1A controls secretory granule biogenesis and trafficking of membrane secretory granule proteins**. *Traffic* 2014, **15**(10):1099-1121.

11. Wang X, Cai Y, Wang H, Zeng Y, Zhuang X, Li B, Jiang L: **Trans-Golgi network-located AP1 gamma adaptins mediate dileucine motif-directed vacuolar targeting in Arabidopsis.** *The Plant cell* 2014, **26**(10):4102-4118.
12. Wang JG, Feng C, Liu HH, Feng QN, Li S, Zhang Y: **AP1G mediates vacuolar acidification during synergid-controlled pollen tube reception.** *Proceedings of the National Academy of Sciences of the United States of America* 2017, **114**(24):E4877-E4883.
13. Park M, Song K, Reichardt I, Kim H, Mayer U, Stierhof Y-D, Hwang I, Jürgens G: **Arabidopsis μ-adaptin subunit AP1M of adaptor protein complex 1 mediates late secretory and vacuolar traffic and is required for growth.** *Proceedings of the National Academy of Sciences* 2013, **110**(25):10318-10323.
14. Feng C, Wang JG, Liu HH, Li S, Zhang Y: **Arabidopsis adaptor protein 1G is critical for pollen development.** In: *Journal of integrative plant biology.* vol. 59; 2017: 594-599.
15. Christensen CA, Subramanian S, Drews GN: **Identification of gametophytic mutations affecting female gametophyte development in Arabidopsis.** *Developmental biology* 1998, **202**(1):136-151.
16. Nordstrom KJV, Albani MC, James GV, Gutjahr C, Hartwig B, Turck F, Paszkowski U, Coupland G, Schneeberger K: **Mutation identification by direct comparison of whole-genome sequencing data from mutant and wild-type individuals using k-mers.** *Nat Biotechnol* 2013, **31**(4):325-+.
17. Zhu Y, Mang H-g, Sun Q, Qian J, Hipps A, Hua J: **Gene discovery using mutagen-induced polymorphisms and deep sequencing: application to plant disease resistance.** *Genetics* 2012, **192**(1):139-146.
18. Schmidt A, Wuest SE, Vijverberg K, Baroux C, Kleen D, Grossniklaus U: **Transcriptome Analysis of the Arabidopsis Megasporocyte Mother Cell Uncovers the Importance of RNA Helicases for Plant Germline Development.** *PLoS biology* 2011, **9**(9):e1001155.
19. Su Z, Zhao L, Zhao Y, Li S, Won S, Cai H, Wang L, Li Z, Chen P, Qin Y et al: **The THO Complex Non-Cell-Autonomously Represses Female Germline Specification through the TAS3-ARF3 Module.** *Current biology : CB* 2017, **27**(11):1597-1609 e1592.
20. Christensen CA, King EJ, Jordan JR, Drews GN: **Megagametogenesis in Arabidopsis wild type and the Gf mutant.** *Sexual plant reproduction* 1997, **10**(1):49-64.
21. Shi DQ, Liu J, Xiang YH, Ye D, Sundaresan V, Yang WC: **SLOW WALKER1, essential for gametogenesis in Arabidopsis, encodes a WD40 protein involved in 18S ribosomal RNA biogenesis.** *The Plant cell* 2005, **17**(8):2340-2354.
22. Borg M, Brownfield L, Twell D: **Male gametophyte development: a molecular perspective.** *Journal of experimental botany* 2009, **60**(5):1465-1478.
23. D'Ippolito S, Arias LA, Casalongue CA, Pagnussat GC, Fiol DF: **The DC1-domain protein VACUOLELESS GAMETOPHYTES is essential for development of female and male gametophytes in Arabidopsis.** *Plant Journal* 2017, **90**(2):261-275.
24. Hafidh S, Fila J, Honys D: **Male gametophyte development and function in angiosperms: a general concept.** *Plant Reproduction* 2016, **29**(1):31-51.
25. Rodriguez-Enriquez MJ, Mehdi S, Dickinson HG, Grant-Downton RT: **A novel method for efficient in vitro germination and tube growth of Arabidopsis thaliana pollen.** *The New phytologist* 2013, **197**(2):668-679.
26. Ozias-Akins P, van Dik PJ: **Mendelian genetics of apomixis in plants.** *Annu Rev Genet* 2007, **41**:509-537.
27. Wang HQ, Liu RJ, Wang JW, Wang P, Shen YH, Liu GQ: **The Arabidopsis kinesin gene AtKin-1 plays a role in the nuclear division process during megagametogenesis.** *Plant Cell Rep* 2014, **33**(5):819-828.
28. Barrett LW, Fletcher S, Wilton SD: **Regulation of eukaryotic gene expression by the untranslated gene regions and other non-coding elements.** *Cellular and molecular life sciences : CMLS* 2012, **69**(21):3613-3634.
29. Pichon X, Wilson LA, Stoneley M, Bastide A, King HA, Somers J, Willis AE: **RNA binding protein/RNA element interactions and the control of translation.** *Curr Protein Pept Sci* 2012, **13**(4):294-304.
30. Bonhomme S, Horlow C, Vezon D, de Laissardiere S, Guyon A, Ferault M, Marchand M, Bechtold N, Pelletier G: **T-DNA mediated disruption of essential gametophytic genes in Arabidopsis is unexpectedly rare and cannot be inferred from segregation distortion alone.** *Mol Gen Genet* 1998, **260**(5):444-452.
31. Meister RJ, Kotow LM, Gasser CS: **SUPERMAN attenuates positive INNER NO OUTER autoregulation to maintain polar development of Arabidopsis ovule outer integuments.** *Development* 2002, **129**(18):4281-4289.
32. Zizoli D, Meyer C, Guhde G, Saftig P, von Figura K, Schu P: **Early embryonic death of mice deficient in γ-adaptin.** *Journal of Biological Chemistry* 1999, **274**(9):5385-5390.

33. Meyer C, Zizioli D, Lausmann S, Eskelinen EL, Hamann J, Saftig P, von Figura K, Schu P: **mu1A-adaptin-deficient mice: lethality, loss of AP-1 binding and rerouting of mannose 6-phosphate receptors.** *The EMBO journal* 2000, **19**(10):2193-2203.
34. Stepp JD, Pellicena-Palle A, Hamilton S, Kirchhausen T, Lemmon SK: **A late Golgi sorting function for *Saccharomyces cerevisiae* Apm1p, but not for Apm2p, a second yeast clathrin AP medium chain-related protein.** *Molecular biology of the cell* 1995, **6**(1):41-58.
35. Kita A, Sugiura R, Shoji H, He Y, Deng L, Lu Y, Sio SO, Takegawa K, Sakaue M, Shunoh H *et al*: **Loss of Apm1, the micro1 subunit of the clathrin-associated adaptor-protein-1 complex, causes distinct phenotypes and synthetic lethality with calcineurin deletion in fission yeast.** *Molecular biology of the cell* 2004, **15**(6):2920-2931.
36. Pagnussat GC, Yu HJ, Sundaresan V: **Cell-Fate Switch of Synergid to Egg Cell in *Arabidopsis eoste* Mutant Embryo Sacs Arises from Misexpression of the BEL1-Like Homeodomain Gene BLH1.** *The Plant cell* 2007, **19**(11):3578.
37. Alvarez J, Smyth DR: **CRABS CLAW and SPATULA, two *Arabidopsis* genes that control carpel development in parallel with AGAMOUS.** *Development* 1999, **126**(11):2377-2386.
38. Clough SJ, Bent AF: **Floral dip: a simplified method for Agrobacterium-mediated transformation of *Arabidopsis thaliana*.** *The Plant journal : for cell and molecular biology* 1998, **16**(6):735-743.
39. Hu B, Jin J, Guo AY, Zhang H, Luo J, Gao G: **GSDS 2.0: an upgraded gene feature visualization server.** *Bioinformatics* 2015, **31**(8):1296-1297.

Tables

Table 1. Segregation of *ap1g2-1^{+/-}* mutation in selfed and reciprocally backcrosses.

Female	Male	Progeny genotypes		
		WT	<i>ap1g2-1^{+/-}</i>	<i>ap1g2-1^{-/-}</i>
<i>ap1g2-1^{+/-}</i>	<i>ap1g2-1^{+/-}</i>	114	123	-
<i>ap1g2-1^{+/-}</i>	WT	44	28	-
WT	<i>ap1g2-1^{+/-}</i>	43	26	-

Table 2. Synchrony of female gametophyte in wild-type and *ap1g2-1^{+/-}* pistils.

Pistil number	No. of FGs at developmental stages in wild-type pistils							No. of FGs at developmental stages in <i>ap1g2-1^{+/-}</i> pistils											
	FG0	FG1	FG2	FG3	FG4	FG5	FG6	FG7	Total FGs	FG0	FG1	FG2	FG3	FG4	FG5	FG6	FG7	No nuclei	Total FGs
P1	44								44	43									43
P2	33	12							45	21	28								49
P3	9	34							43	1	25	39							65
P4	36	2							38	1	25	3	9						38
P5	39	15	2	1					57	22	1	13	5				1	5	47
P6	25	10	4						39	22	1	6	12				1	5	47
P7	13	17	9	1					40	18	2	7	7	3				6	43
P8	9	6	26	10					51	17	2	3	3	3	4	4	4	6	42
P9		1	15	3	6	10			35	23		2	1		4	14	6		50
P10			11	10	11	10			42	18					3	18	9		48
P11				3	50	52			18						1	21	10		50
P12					51	51			17							20	19		56
P13					49	49			6							24	19		49
P14					50	50			5							21	20		46

Table 3 Synchrony of female gametophyte in *ap1g2-3^{-/-}* and *ap1g2-4^{-/-}* pistils

Pistil number	No. of female gametophytes at developmental stages in <i>ap1g2-3^{-/-}</i> pistils							No. of female gametophytes at developmental stages in <i>ap1g2-4^{-/-}</i> pistils												
	FG0	FG1	FG2	FG3	FG4	FG5	FG6	FG7	No nuclei	Total FGs	FG0	FG1	FG2	FG3	FG4	FG5	FG6	FG7	No nuclei	Total FGs
P1	41									41	50									50
P2	18	28								46	40	11								51
P3	1	36	1						5	43	6	37	2							45
P4	1	35	1						9	46	10	35	1							46
P5	1	45	1						9	56	28	3	7						6	44
P6		29	3						3	35	7	2	7	10					19	45
P7		30	2	4					7	43	7	4	11	10	1				18	51
P8		32	2	2	4				9	49	2		6	8	7	4			20	47
P9		16	1	1	3	3	1	1	10	36	7		5	11	3	4	3	12	45	
P10		27		1	3	1	1	2	19	54	3		7	7	2	2	13	13	47	
P11		21	1		1	2		2	16	43	7	1	1		2	17	27	55		
P12		21			1	2	5	5	15	49	6		2		1	4	9	25	47	
P13		16				1	1	12	20	50	5				1	2	15	21	45	
P14		15					1	10	23	49	6						19	26	51	

Table 4. List of phenotypes of three *ap1g2* alleles

Name	Mutant site	Phenotype observed
<i>ap1g2-1^{+/+}</i>	T-DNA insertion in 7 th exon	About 50% female gametophytes arrested at stage FG1 and about 46.04% male gametophytes arrested before PM1
<i>ap1g2-3^{-/-}</i>	T-DNA insertion in 3'UTR	77.75% female gametophytes arrested at stage FG1 and about 49.71% male gametophytes arrested before PM1
<i>ap1g2-4^{-/-}</i>	Multiple mutantions including a base change in 7 th exon	57.30% female gametophytes arrested at stage FG1; outer integuments development arrested; seeds malformed; big flowers

Figures

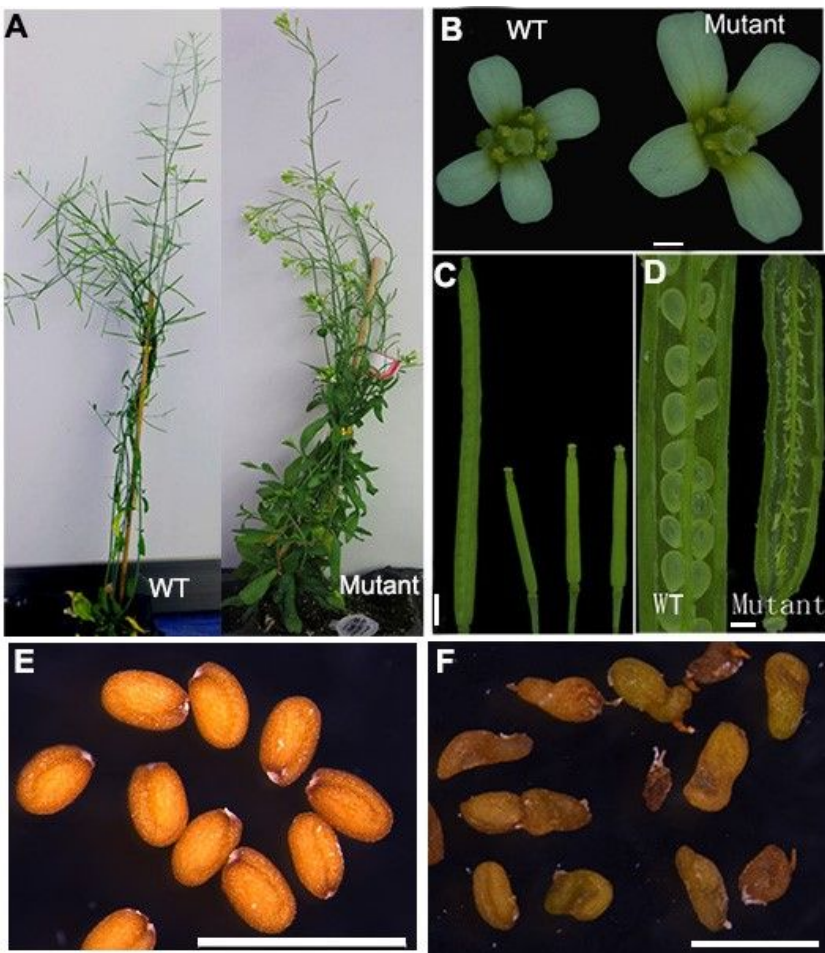


Figure 1

Phenotypes of EMS-induced sterile mutant. (A) The phenotypic variation between wild-type (WT) and EMS-induced mutant plant. (B) The wild-type flowers are smaller than mutant flowers. (C) Comparison in mature silique length of the wild type and mutant (D) The open siliques of the wild type have normal seed setting and mutant have aborted seeds. (E) Seeds of WT. (F) Seeds of mutant after two rounds of backcrosses. Bar=0.5 cm in B and D; 1 cm in C, E and F.

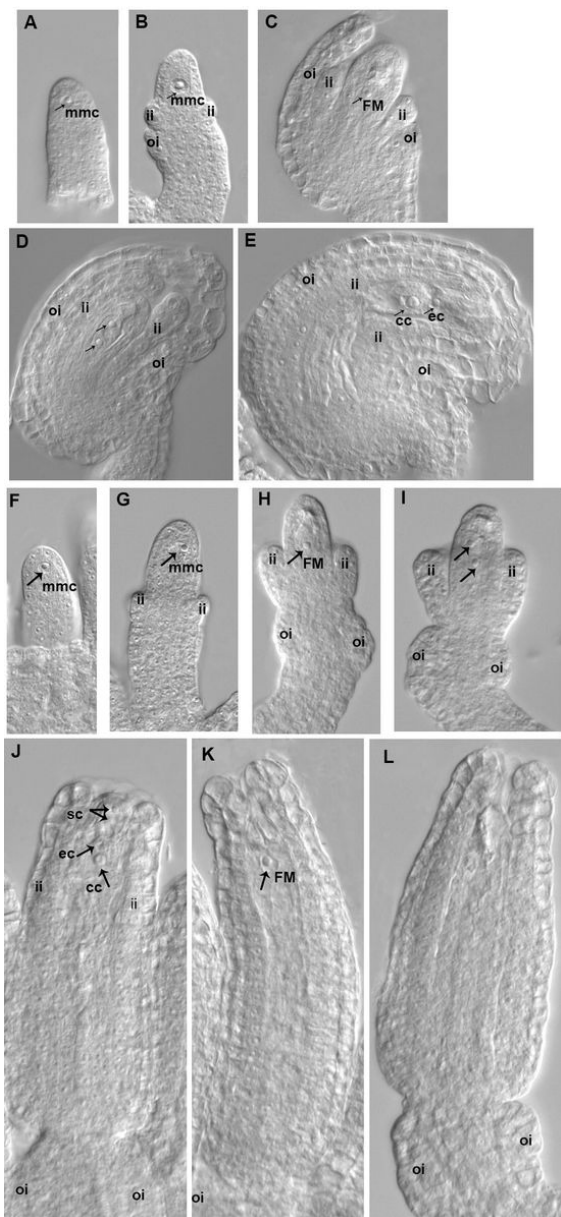


Figure 2

ovule development in WT and the EMS-induced sterile mutant. (A- E) ovule development in WT. (A) Ovule primordium showing a megasporocyte (mmc). (B) Stage 2- \ddagger when the outer integument initiated. (C) Stage FG1. (D) Stage FG3. (E) Stage FG7. (F-L) Ovule development in the mutant. (F) Ovule primordium showing a megasporocyte (mmc); (G) ovule at stage 2- \ddagger without outer integuments initiation; (H) Ovule at stage FG1 with abnormal integuments; (I) Stage FG3. (J-L) Stage FG7; ii, inner integuments; oi, outer integuments; mmc, megasporocyte; FM, functional megasporocyte; cc, central cell; ec, egg cell; sc, synergid cells.

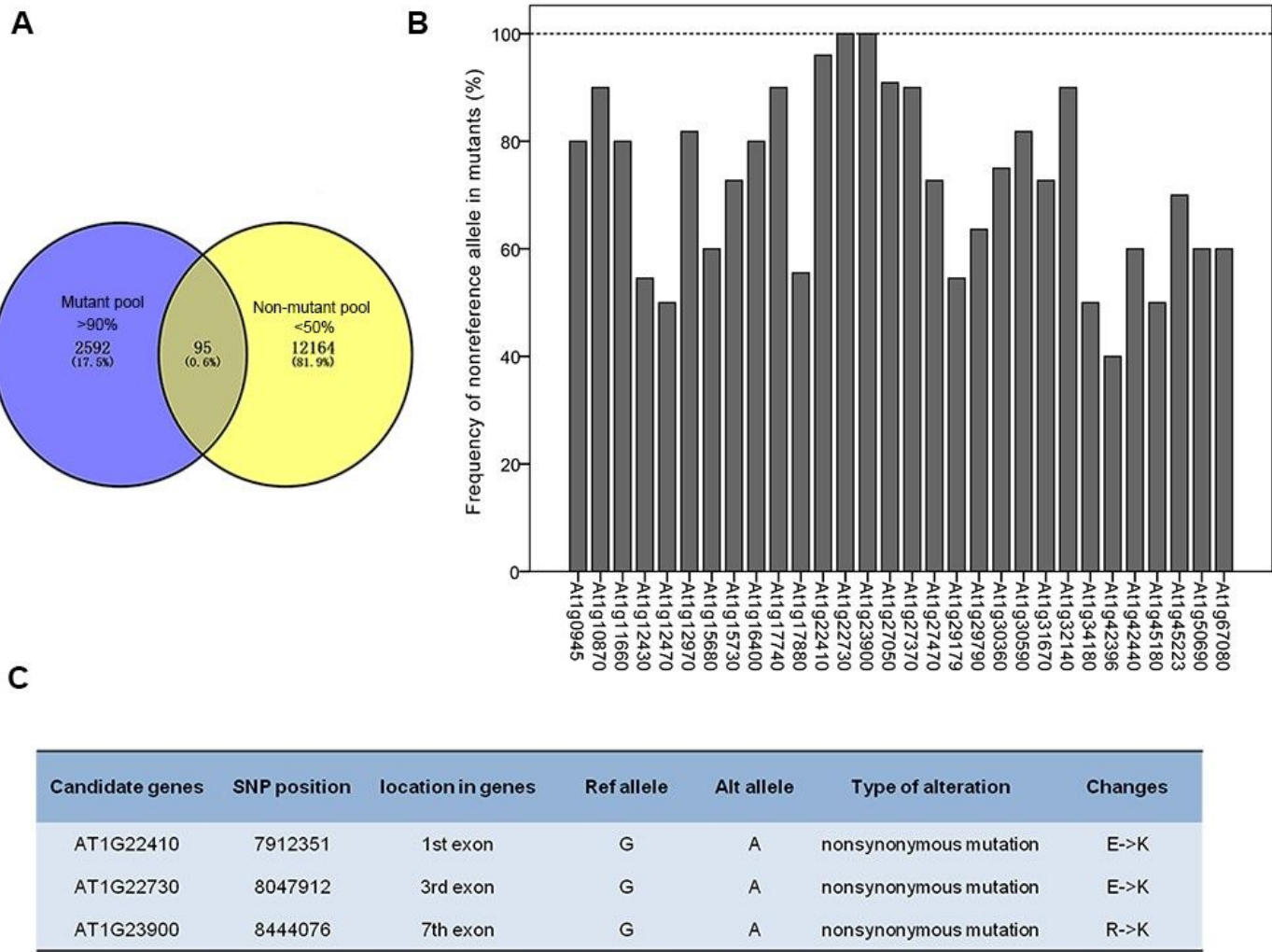
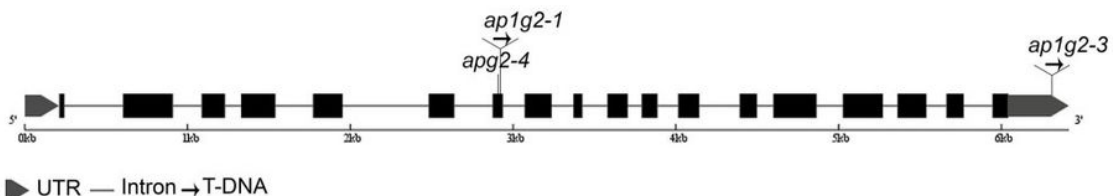
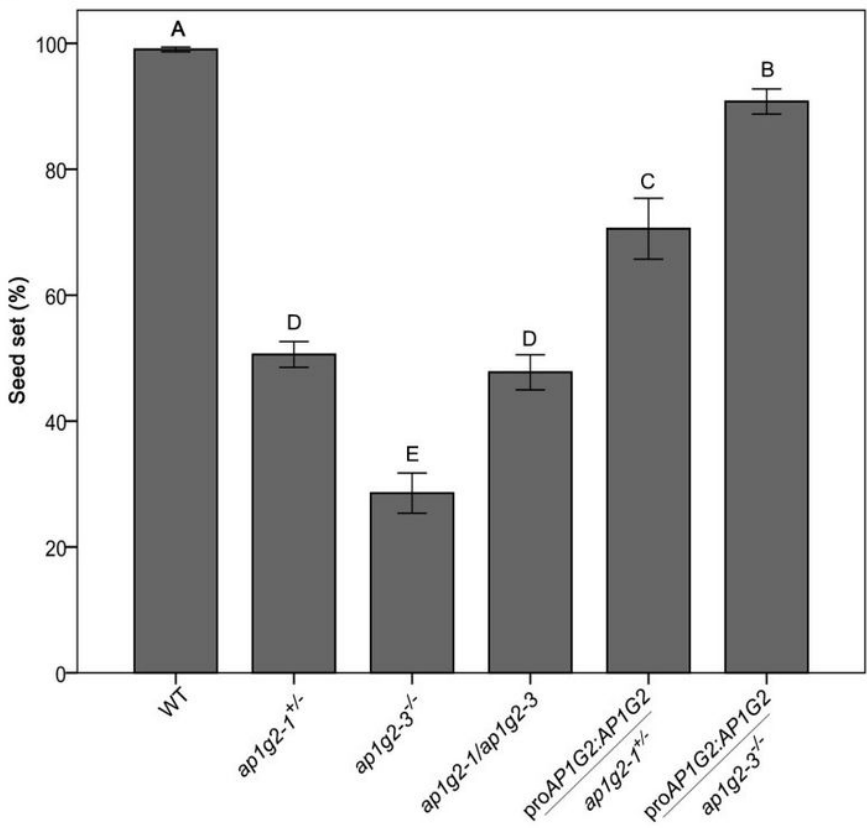


Figure 3

Identification of candidate genes. (A) The number of candidate SNPs. 95 candidate SNPs with the non-reference allele > 90% frequency in the mutant pool and < 50% in the non-mutant pool. (B) Frequency of non-reference allele in mutants of BC2 progeny. (C) Annotation of candidate SNPs and associated genes. Shown are candidate genes, the base position, sequence of the reference allele, sequence of the non-reference allele, type of alteration, and predicted amino acid change for each SNP.

A**B****C****Figure 4**

(A) Schematic [39] representation of the gene AP1G2 with the positions of the various T-DNA insertions (*ap1g2-1* and *ap1g2-3*) and EMS mutant harboring a G-to-A base change at nucleotide position 8444076 (*ap1g2-4*). (B) *ap1g2* fruits contain aborted ovules and are shorter than those of the wild type and complementation lines of the *ap1g2-1^{+/−}* and *ap1g2-3^{−/−}* mutant. (C) Quantification of seed set in siliques of *ap1g2-1^{+/−}*, *ap1g2-3^{−/−}*, *apg2-1/apg2-3* mutants, wild-type plants, and genetic complementation lines of *ap1g2-1^{+/−}* and *ap1g2-3^{−/−}*. Error bars indicate standard error. The capital letters above the bars mean very significant difference with the wild type ($P<0.01$).

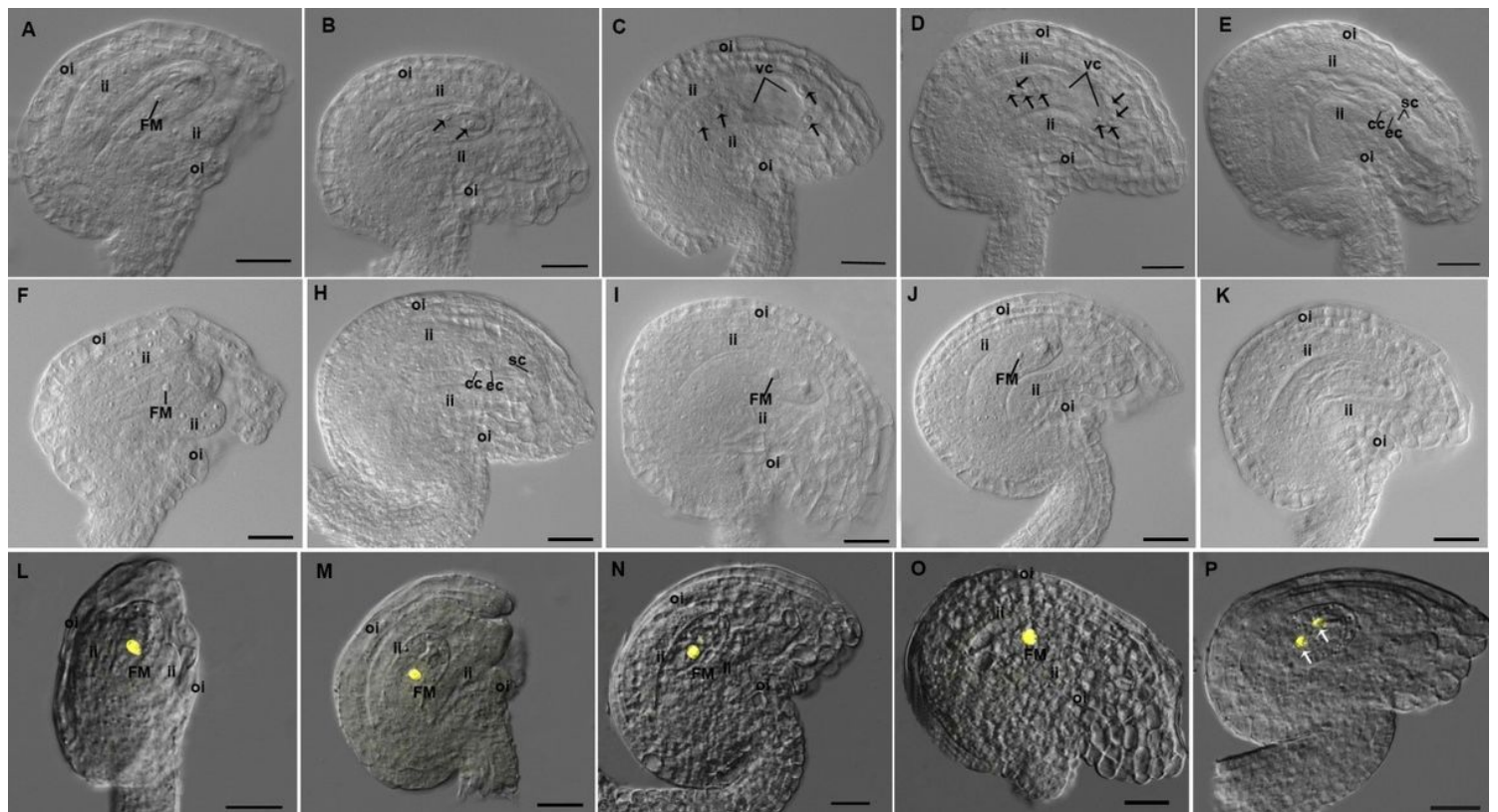


Figure 5

Female gametogenesis is impaired in ovules from *ap1g2-1+/-* and *ap1g2-3-/-* plants. (A-E) Ovule development in the wild type, stage FG1 (A); stage FG3 (B); stage FG4 (C); stage FG5(D); stage FG7 (E). (F-J) Ovules in *ap1g2-3-/-*, normal ovule at stage FG1 (F); aborted mature ovule (G I); aborted ovules arrested at FG1; (J) Aborted ovules with functional megasporangium degenerated. (K-N) Analysis of H2B-YFP expression under the control of the AKV promoter in *ap1g2-1+/-* indicating one gametophytic cell. (P) YFP signals in the wild type at FG2. Scale bars are 20 μ m, ii, inner integuments; oi, outer integuments; FM, functional megasporangium; cc, central cell; ec, egg cell; sc, synergid cells.

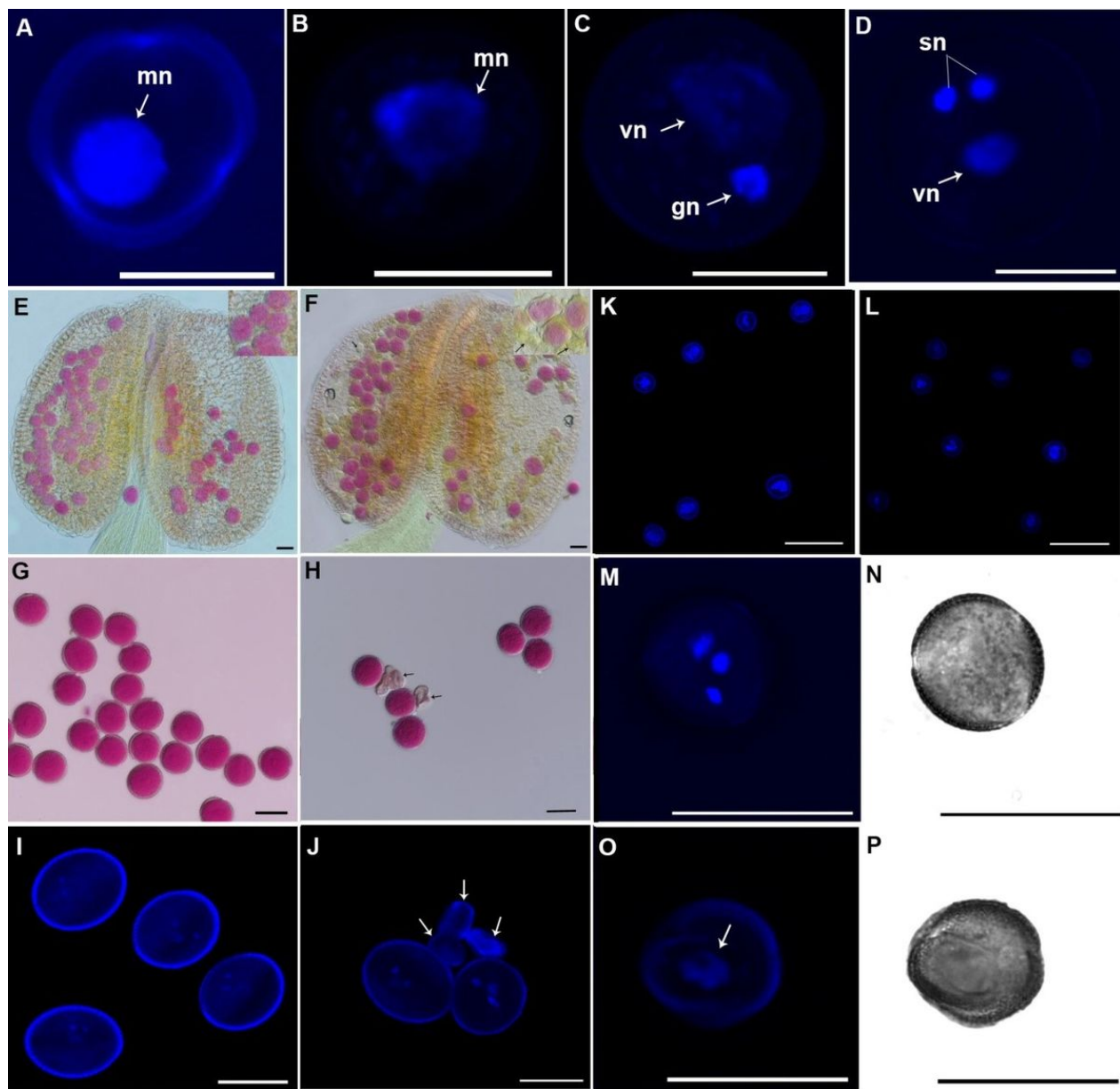


Figure 6

Pollen development was impaired in *apg2-1+/-* mutants. (A-D) The nuclear constitution of WT pollen grains through microgametogenesis developmental stages. Nuclei are indicated by arrows, mn, microspore nucleus; vn, vegetative nucleus; gn, generative nucleus; sn, sperm nuclei. Bars = 10 µm. (E, F) Pollen viability by means of Alexander's staining in anthers from WT and *apg2-1+/-* respectively. Arrows indicate impaired pollen grains. (G, H) Alexander's staining of mature pollen grains from WT and *apg2-1+/-*, respectively. Arrows indicate impaired pollen grains. (I, J) 40,6-Diamidino-2-phenylindole (DAPI) staining of pollen grains from buds at stage 13 in WT and *apg2-1+/-* respectively. Arrows indicate impaired pollen grains. (K, L) DAPI staining of microspores from buds at stage 9 in WT and *apg2-1+/-* respectively. (M, O) Nuclear constitution by means of DAPI staining in pollen grains in buds at stage 12 from WT and *apg2-1+/-*, respectively. Nuclei are indicated by arrows. (N, P) Bright field images of (I) and (K), respectively. Bars = 20 µm in E-P.

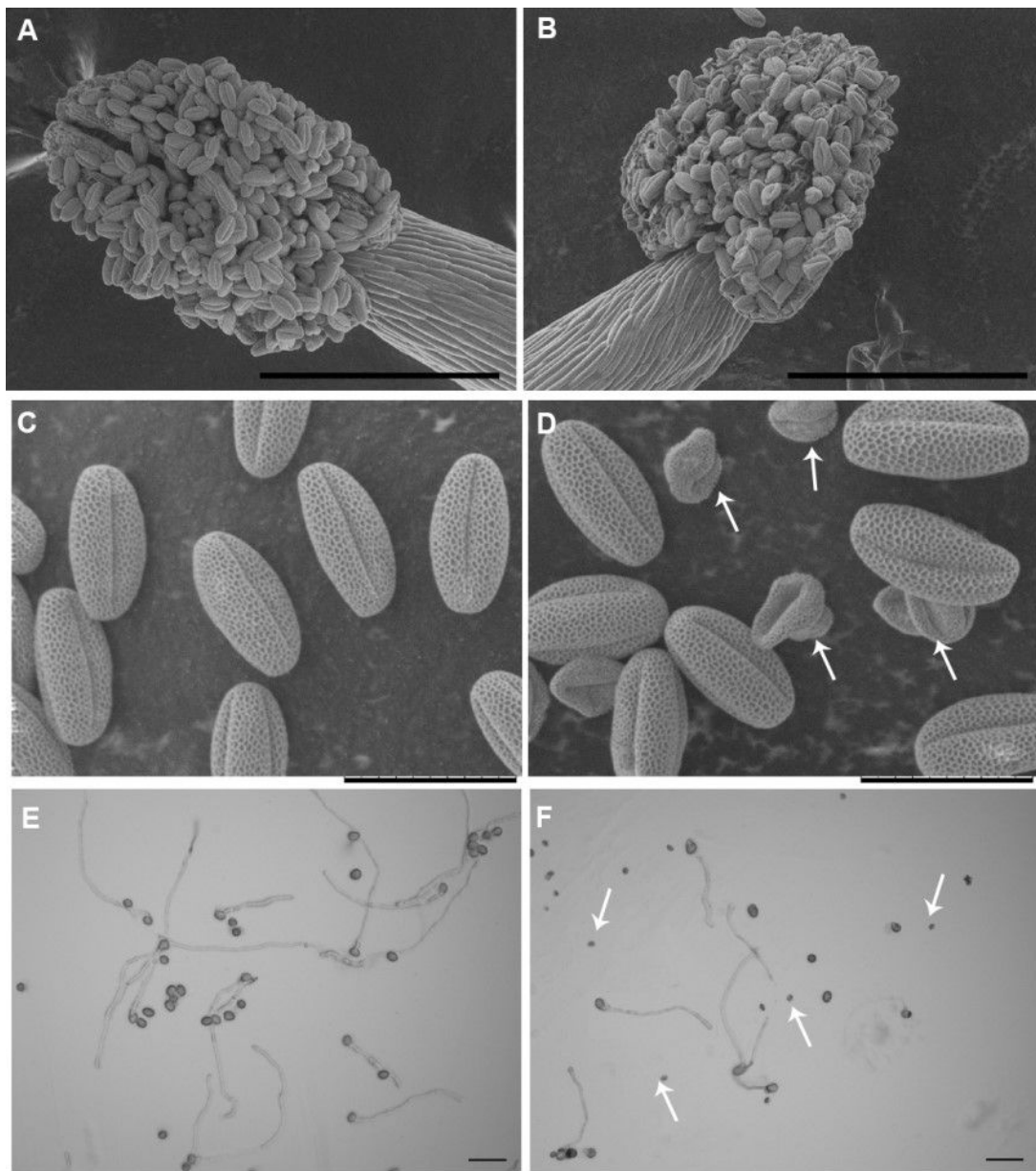


Figure 7

Pollen development was impaired in *apg2-3-/-* mutants. (A, B) Scanning electron micrographs (SEMs) of anthers from WT and *apg2-3-/-*, bars = 200 μ m. (C, D) SEMs of pollen grains from WT and *apg2-3-/-*, bars = 30 μ m. (E, F) Pollen grains germination in vitro of WT and *apg2-3-/-*, respectively, bars = 100 μ m. Arrows point at aborted pollen grains.

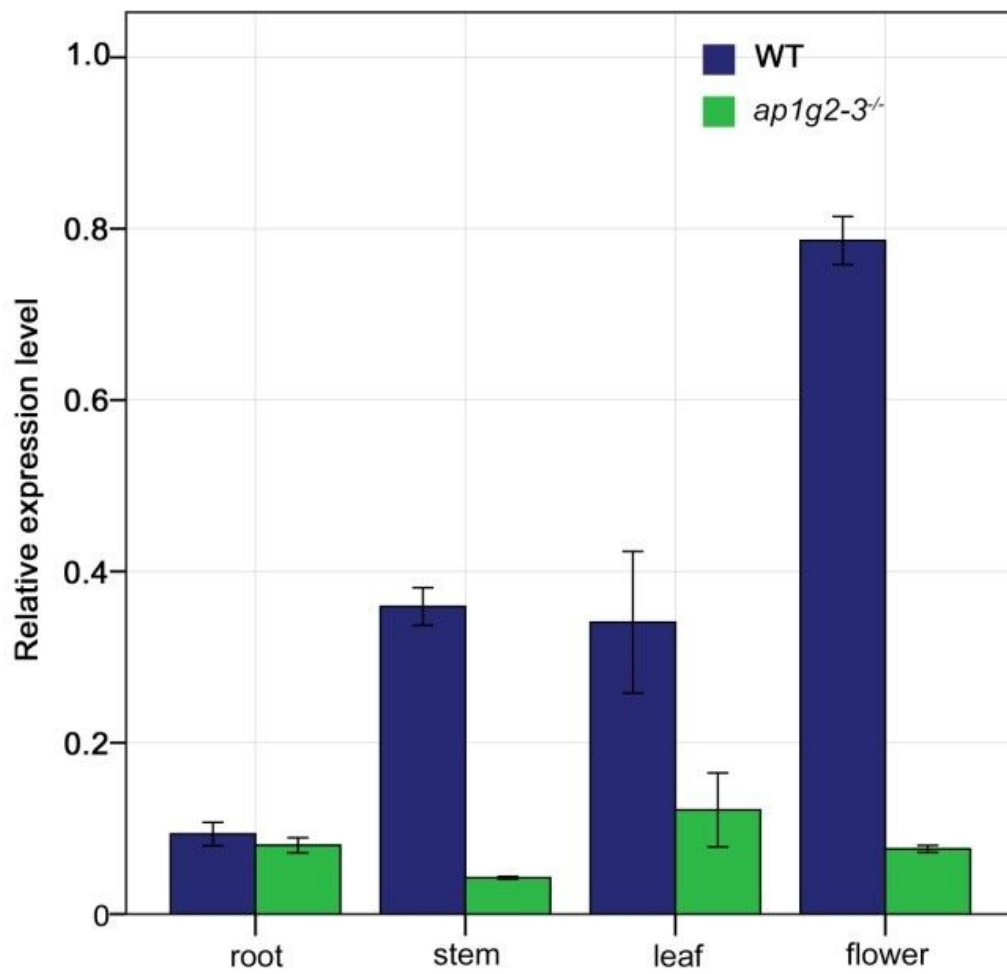


Figure 8

Quantitative qRT-PCR analysis of the AP1G2 gene expression. Each result was the average of three independent biological replicates. Error bars indicate standard error.

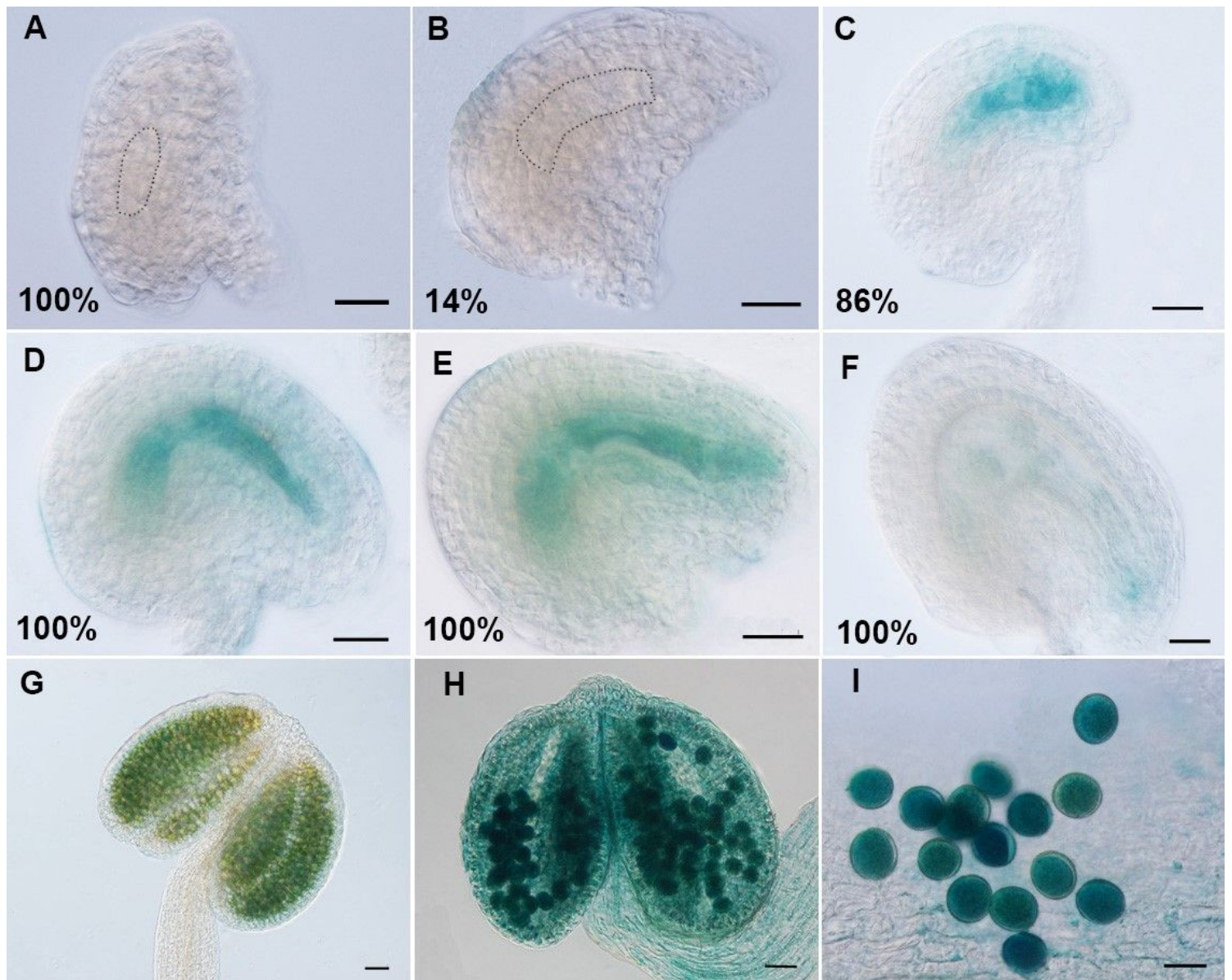


Figure 9

Activity of AP1G2 in ovules and anthers. (A-F) GUS staining in ovules: 100% of ovules containing female gamete before stage FG3 and 14% of ovules containing female gametophyte at FG4 or FG5 were not detected GUS expression (A-B); ovules containing female gametophyte at FG4 to 7 with GUS staining (C-E), GUS staining reduced in embryogenesis (F). (G-I) GUS staining in anthers and pollen grains. Number means the percentage of ovules either stained by GUS or not. Bars = 20 μ m. 0 μ m in D, F, H.

Supplementary Files

This is a list of supplementary files associated with this preprint. Click to download.

- [Figures.docx](#)